Supplementary Material (ESI) for Chemical Communications

Electronic Supplementary Information

Effects of particle size on surface electronic and electrocatalytic properties of Pt/TiO_2 nanocatalysts

Sung Jong Yoo,[a] Tae-Yeol Jeon,[a] Kug-Seung Lee,[a] Kyung-Won Park,[b] and Yung-Eun Sung*[a]

[a]School of Chemical and Biological Engineering, Seoul National University, Shinlimdong 56-1, Seoul 151-742, Korea.

[b]Department of Chemical and Environmental Engineering, Soongsil University, Seoul 156-743, Korea.

*E-mail: ysung@snu.ac.kr

1. Experimental

Pt/TiO_2 nanocatalyst electrodes were grown using an RF magnetron co-sputtering system which consisted of a dual sputtering-gun. Si (100) and glassy carbon were used as the substrates to characterize the structural and electrochemical properties, respectively. Pt and TiO_2 were used as the target materials. In order to fabricate the Pt/TiO_2 nanocatalyst electrodes, co-sputtering was used with different RF powers. Co-sputtering was performed under inert Ar gas at a flow rate of 26 SCCM at room temperature for 10 minutes, which produced films about 100 nm thick. In order to fabricate the Pt/TiO_2 nanocatalyst electrodes with various sizes, the RF power of the guns used with the metal targets in the RF magnetron sputtering system was adjusted. A pure Pt electrode was also produced. X-ray diffraction (XRD) (MAC Science M18XHF-SRA equipped with a Cu Kα source at 30 kV-30 mA) analyses of the as-prepared electrodes were used to determine their degree of crystallinity. The Pt L_{III} edge X-ray absorption spectra were recorded using the 7C beam line at the Pohang

Light Source (PLS) with a ring current of 120~170 mA at 2.5 GeV. A Si (111) monochromatic crystal was used with detuning of the intensity to 80 % to eliminate high-order harmonics. The data were collected in fluorescence and transmission modes. Energy calibrations were carried out for all measurements by using Pt foil placed in front of the third ion chamber and assigning the first inflection point to 11564 eV. *In situ* XANES measurements were conducted using an electrochemical cell designed for acquiring good absorption spectra without compromising the electrochemistry (see Fig. S1). The working electrode composed of Pt/TiO_2 nanocatalysts was deposited on a conductive carbon paper (TGPH-060, Toray) which was connected to the out circuit through a Pt foil. The counter electrode was a carbon paper (TGPH-060, Toray). A proton exchange membrane (Nafion 212, DuPont Chemical Co.) separated the working and counter electrodes. An electrolyte consisting of 0.1 M $HClO_4$ (HPLC grade, Sigma-Aldrich) was added to the cell to increase the wetting of the sample. It did not affect the measurements, because of its low X-ray absorption and anion adsorption characteristics. The data analysis package used for XANES was the University of Washington's data analysis program. The XANES spectra were first subjected to background removal by fitting the pre-edge data to a Victoreen type formula over the range of 200 to 80 eV below the edge, followed by extrapolation over the energy range of interest and subtraction from the data. After the removal of the background contributions, the spectra were corrected for edge-shifts using the second derivatives of the inflection points of the data from the reference channel. The procedures used for normalization were the conventional ones. The normalization value was chosen as the absorbance at the inflection point of one EXAFX oscillation. The spectra were thus normalized by dividing each datum point by the normalization value. The spectral window for such an integration was -10 to 13 eV, relative to the absorption edge.

An AutoLab PGSTAT20 potentiostat and rotating disk electrode (RDE) system

(Ecochemie) with a conventional three electrode configuration were used for all of the electrochemical measurements. All of the electrochemical measurements, except for the MOR with the RDE configuration, were performed in Ar purged 0.1 M $HClO_4$ solution. For the MOR experiment, 99.99% Ar gas was bubbled into the electrolyte for 10 min before each measurement. A catalyst coated glassy carbon electrode with a diameter of 5 mm was used as the working electrode. Before each measurement, the glassy carbon electrode was polished with 0.05 micrometer alumina paste, followed by washing with DI water in an ultrasonic bath. A saturated calomel electrode (SCE) with 3 M KCl (Gamry) and glassy carbon rod were used as the reference and counter electrodes, respectively. However, in this paper, all of the potentials were reported with respect to the NHE.

For the CO-bulk oxidation, 0.1 M $HClO_4$ electrolyte was purged with CO gas at a constant electrode potential of 0.05 V verse NHE for 30 min. After the saturation of CO gas, the potential was cycled 5 times between 0.05 and 1.0 V with 50 mV s^{-1}, at 1600 rpm. The stable 10 sweep was recorded with 1 mV s^{-1} and 1600 rpm in the same potential region. After the reactions of interest were studied, a cyclic voltammogram was recorded at 298 K and was compared to the initial one to analyze eventual changes of the surface.

2. Pt nanoparticles formation

When the Pt was deposited by the conventional sputtering method, the atoms that arrived at the substrate diffused and formed islands, due to their tendency to strongly bind to each other rather than to the substrate. This coalescence of islands then leads to the formation of smooth films. In contrast, when the Pt was simultaneously co-sputtered with the metal oxide, thermodynamically stable phase separation occurred between Pt and the metal oxide and the coalescence of Pt islands was limited, due to the presence of the metal oxide, thus leading to the formation of new types of electrodes composed of Pt nanoparticles embedded in the metal

oxide phase, as shown in Fig. S2. This new electrode fabrication system enables the Pt nanoparticles to be homogeneously dispersed on the supporting materials and their size to be readily controlled. The formation of a Pt nanoparticle phase embedded in the metal oxide was confirmed from the TEM images.

3. Analysis of Pt/TiO_2 nanocatalysts electrodes

The size uniformity of the Pt nanoparticles in the TiO_2 matrix fabricated using the dual-gun sputtering system was demonstrated by means of the TEM images shown in Fig. S3a. The dark points and bright region correspond to the Pt nanoparticles (~2 nm) and TiO_2 matrix, respectively. The presence of well-dispersed Pt nanoparticles embedded in the TiO_2 matrix is also confirmed by the image in Fig. S3b. The crystalline plane of the Pt nanoparticles, representing the d-spacing of the (111) plane (d_{111} ~ 0.227 nm), can be observed in the high-resolution TEM image of Fig. S3c, which is in agreement with the value for crystalline Pt. As shown in the transmission electron diffraction (TED) pattern in Fig. S3d, the Pt nanoparticles in the TiO_2 matrix do not consist of a Pt oxide phase, but rather have excellent crystallinity, in spite of their concomitant deposition by the dual-gun sputtering method. The formation of crystalline Pt is also confirmed by the TED analysis of the (111), (200), (220), (311), (222), and (400) planes. Energy dispersive X-ray spectroscopy (EDX) analysis was carried out in order to obtain information on the chemical properties of Pt/TiO_2. The EDX spectroscopy analysis indicated that only Pt and TiO_2 were present and that the ratio of Pt to TiO_2 was 1:1.7 (Fig. S3e). The presence of crystalline Pt and amorphous TiO_2 is also confirmed by the XRD patterns shown in Fig. S3f and the average size of the Pt nanoparticles is about 2 nm, as calculated using the Debye-Scherrer equation.[1]

Fig. S5 shows cyclic voltammograms in 0.1 M $HClO_4$ for the size-controlled Pt/TiO_2 nanocatalysts. The voltammograms of the Pt/TiO_2 nanocatalysts exhibit the characteristic

features of clean polycrystalline Pt.[2] Two reversible hydrogen adsorption/desorption peaks are clearly identified in the potential region from +50 to +250 mV.

The catalytic activity of the Pt catalyst is usually evaluated by measuring its active surface area. The electrochemical surface area of a Pt catalyst is usually determined by the hydrogen underpotential deposition (H-UPD) method. The H^+ adsorption charge density was evaluated by integrating the cathode current for the hydrogen adsorption reaction while correcting for the double-layer charging current. For a polycrystalline Pt electrode, the charge associated with the above reaction is 210 μC cm^{-2}.[3] The electrochemically active specific surface areas of the 1.5 nm and 2 nm sized nanocatalysts are 1.6 and 2.0 times as large as that of the 4 nm sized nanocatalyst, as expected from their different morphologies and the coverage of platinum shown in Fig. S4.

4. Stability of Pt/TiO_2 nanocatalysts electrodes

The catalytic stability of the Pt/TiO_2 nanocatalysts was examined using chronoamperometry. Fig. S11 shows the chronoamperometry curves recorded at 0.5 V in a solution containing both CH_3OH and $HClO_4$. Compared with the Pt thin film, the 3 nm Pt/TiO_2 nanocatalysts exhibited a slower current decay over time, indicating their higher tolerance to CO-like intermediates than the Pt thin film. However, the current decay with time for the 1.5 nm and 4 nm samples was close to that of the Pt thin film; thus, no stability gain was achieved for these two samples.

5. References

1. V. Radmilvic, H. A. Gasteiger, P. N. Ross, *J. Catal.*, 1995, **154**, 98.
2. B. Gollas, J. M. Elliott, P. N. Bartlett, *Electrochim. Acta*, 2000, **45**, 3711.
3. J. Wang, G. M. Swain, *J. Electrochem. Soc.*, 2003, **150**, E24.

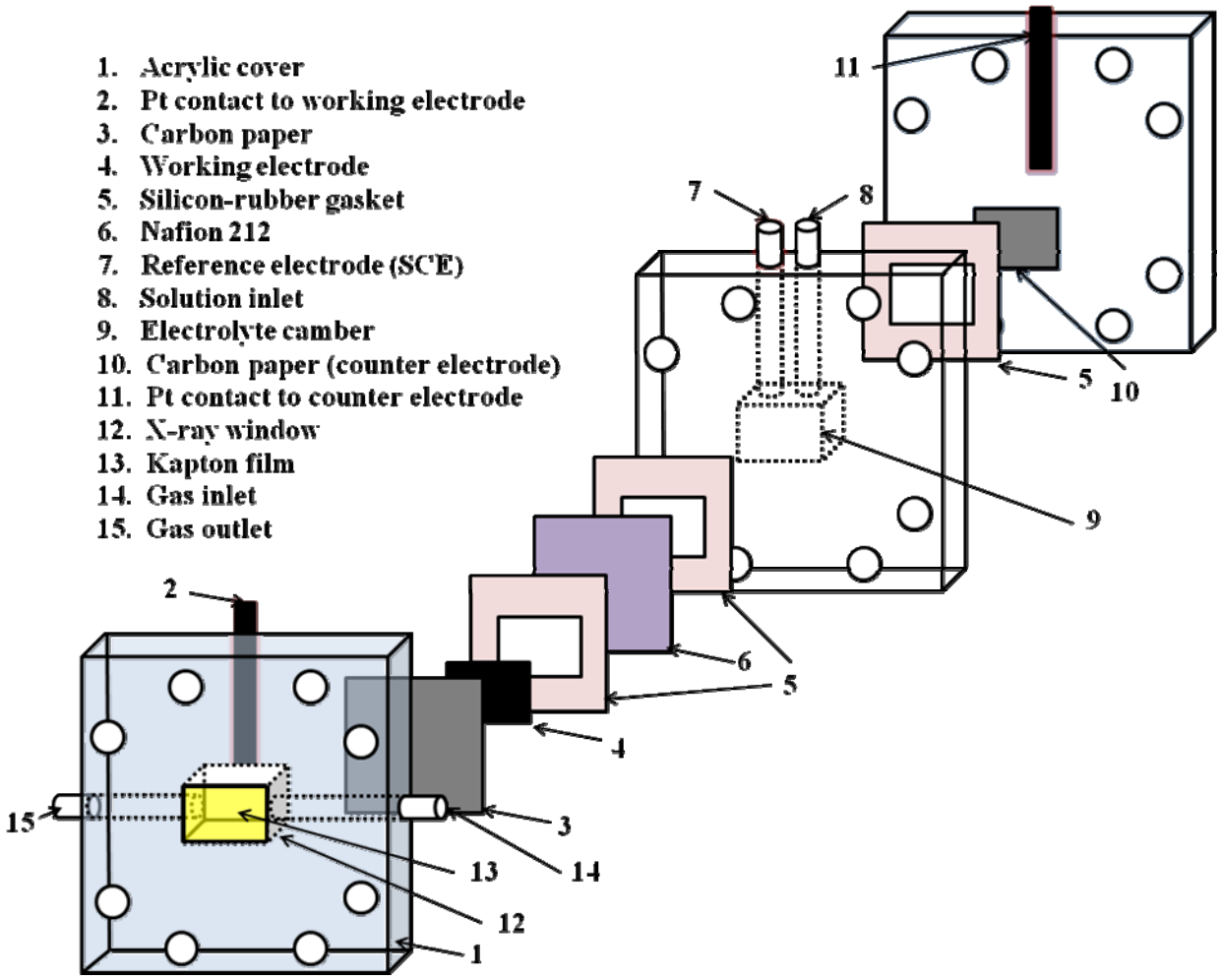

Figure S1. Schematic diagram of the *in situ* electrochemical cell used to obtain the XANES spectra.

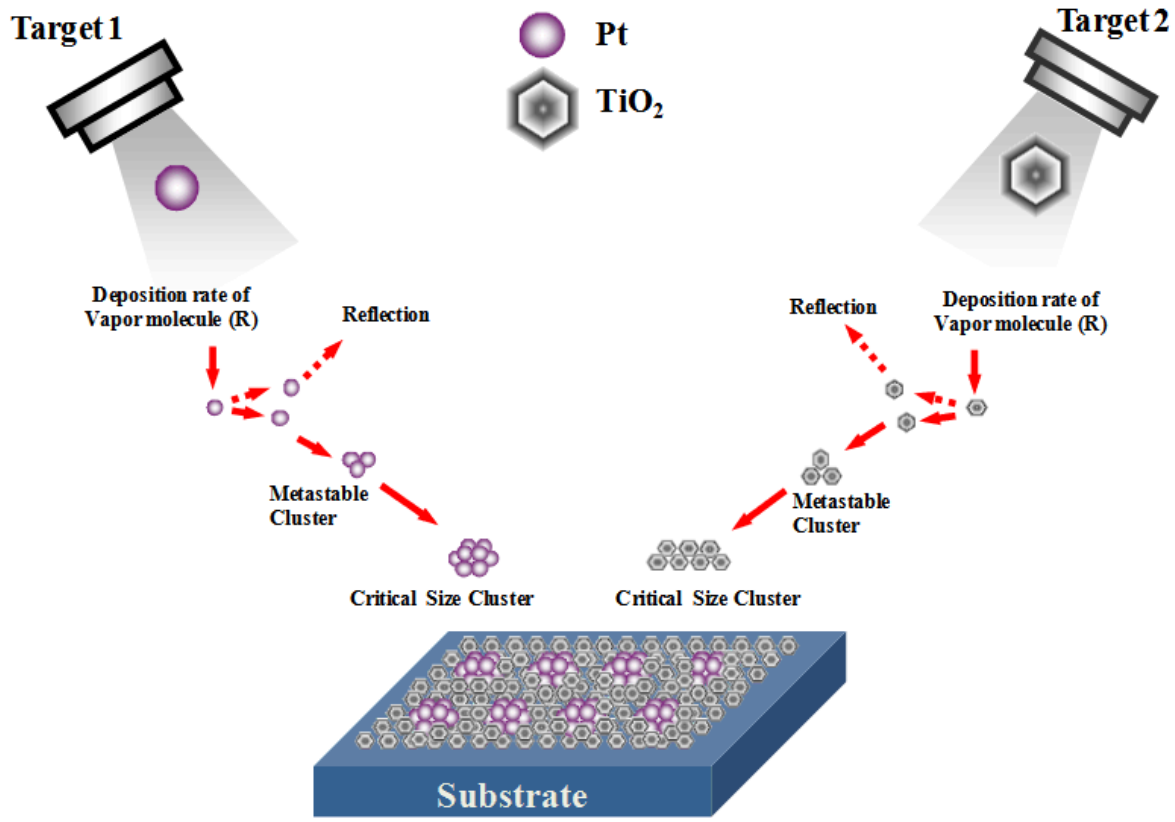

Figure S1. Schematic sized-controlled growth process of the Pt nanoparticles embedded in the metal oxide using a dual-gun sputtering system.

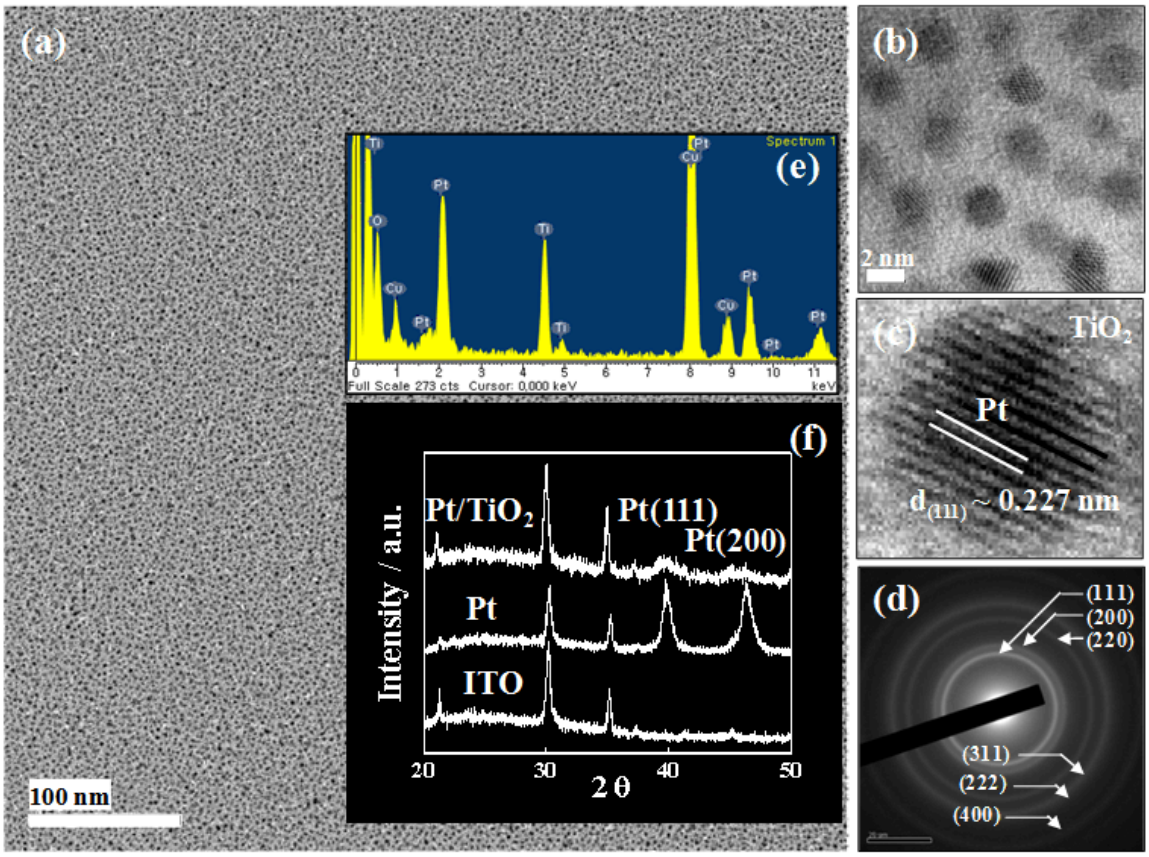

Figure S2. (a) Low-resolution, (b), (c) high-resolution TEM images, (d) TED pattern, (e) EDX data, and (f) XRD pattern of 2 nm sized Pt nanoparticles embedded in TiO_2 matrix.

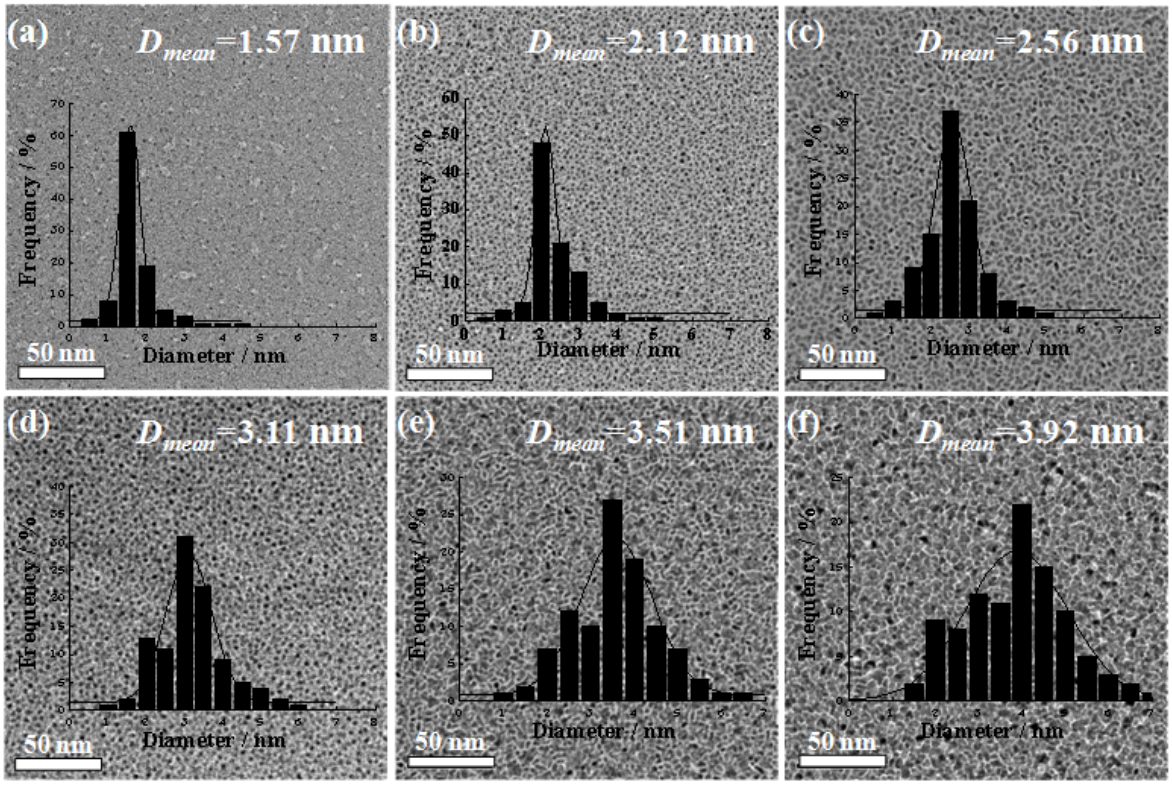

Figure S3. Particle size distribution obtained from the TEM images for the Pt/TiO_2 s nanocatalysts with Pt particle sizes of (a) 1.57 nm, (b) 2.12 nm, (c) 2.56 nm, (d) 3.11 nm, (e) 3.51, and (f) 3.92 nm.

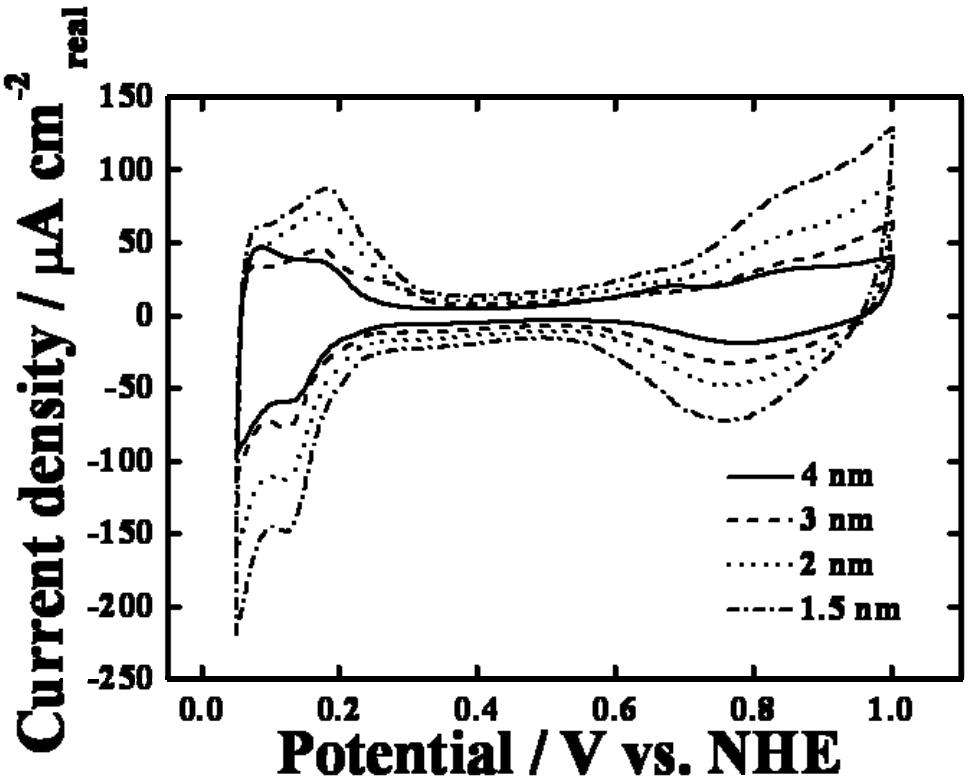

Figure S4. Cyclic voltammograms of the catalysts recorded in 0.1 M $HClO_4$ at 298 K with a scan rate of 50 mV s^{-1}.

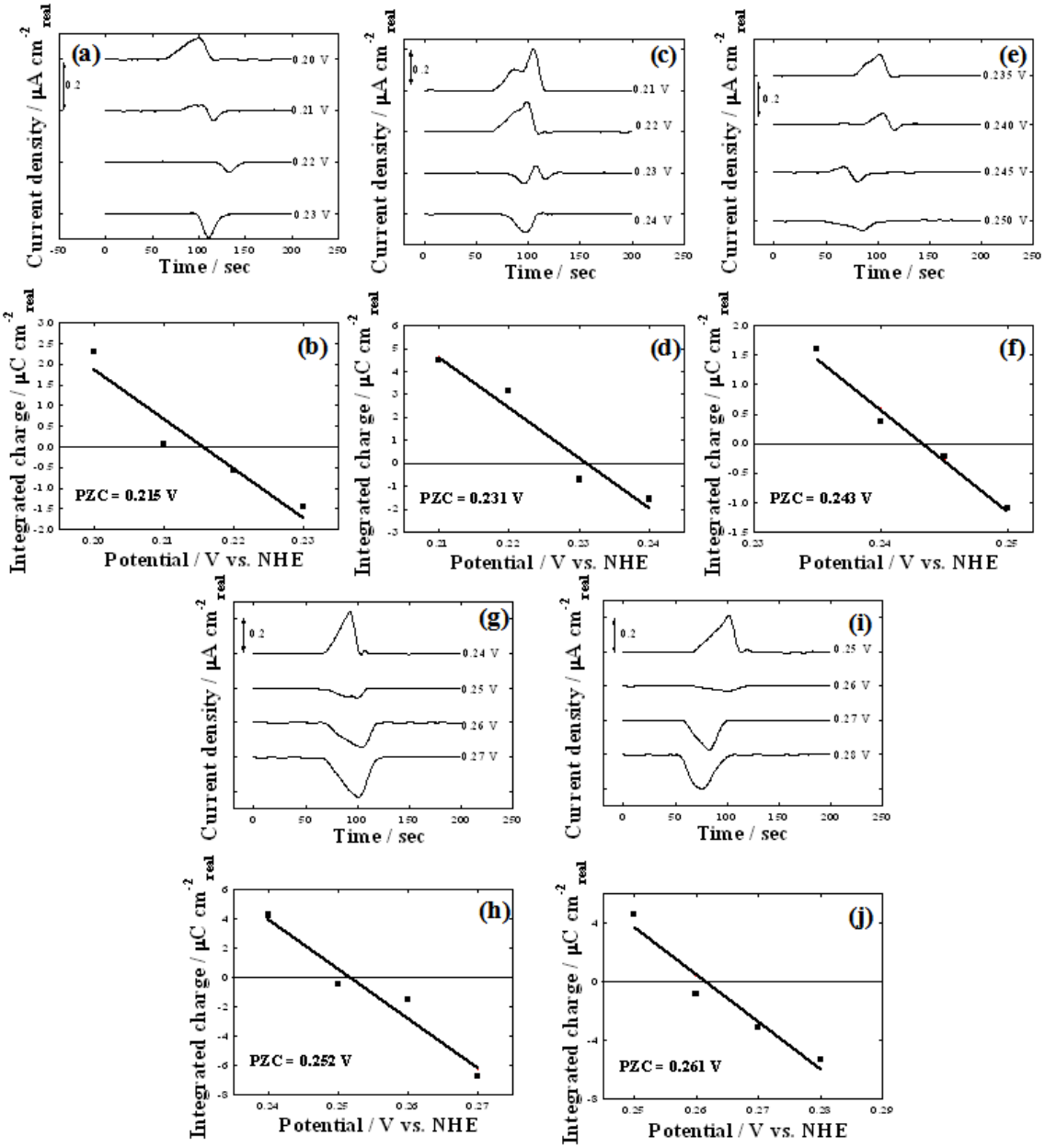

Figure S5. CO-displacement method for determining the PZTC of Pt/TiO_2 nanocatalysts. Displacement charge versus time after introducing CO into the system (a), (c), (e), (f), and (i) measured in 0.1 M $HClO_4$ at 298 K with a rotation rate of 1600 rpm. The individual curves are offset from zero for clarity. (b), (d), (f), (h), and (j): Integrated charge under the CO-displacement peak versus the applied potential. The PZTC corresponds to the potential where the regression line crosses zero.

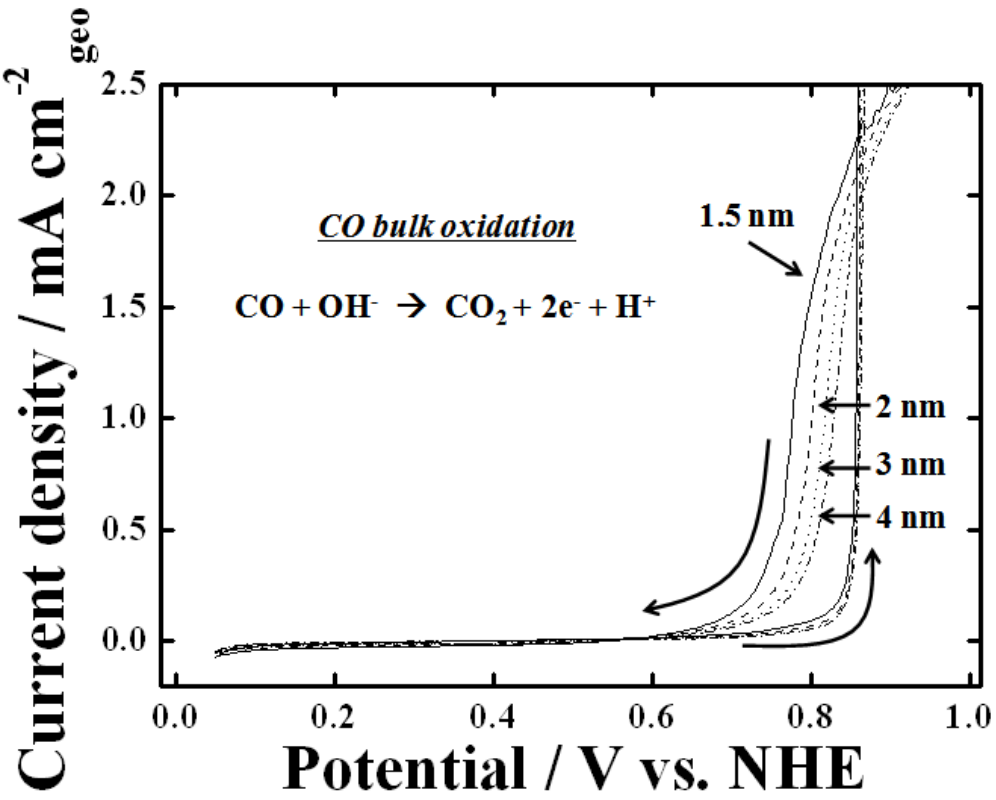

Figure S7. Comparison of the CO bulk oxidation on the 1.5 ~ 4 nm Pt nanocatalysts in the negative sweep (1600 rpm, 1 mV s^{-1}) from 1 V where the surface is covered with OH.

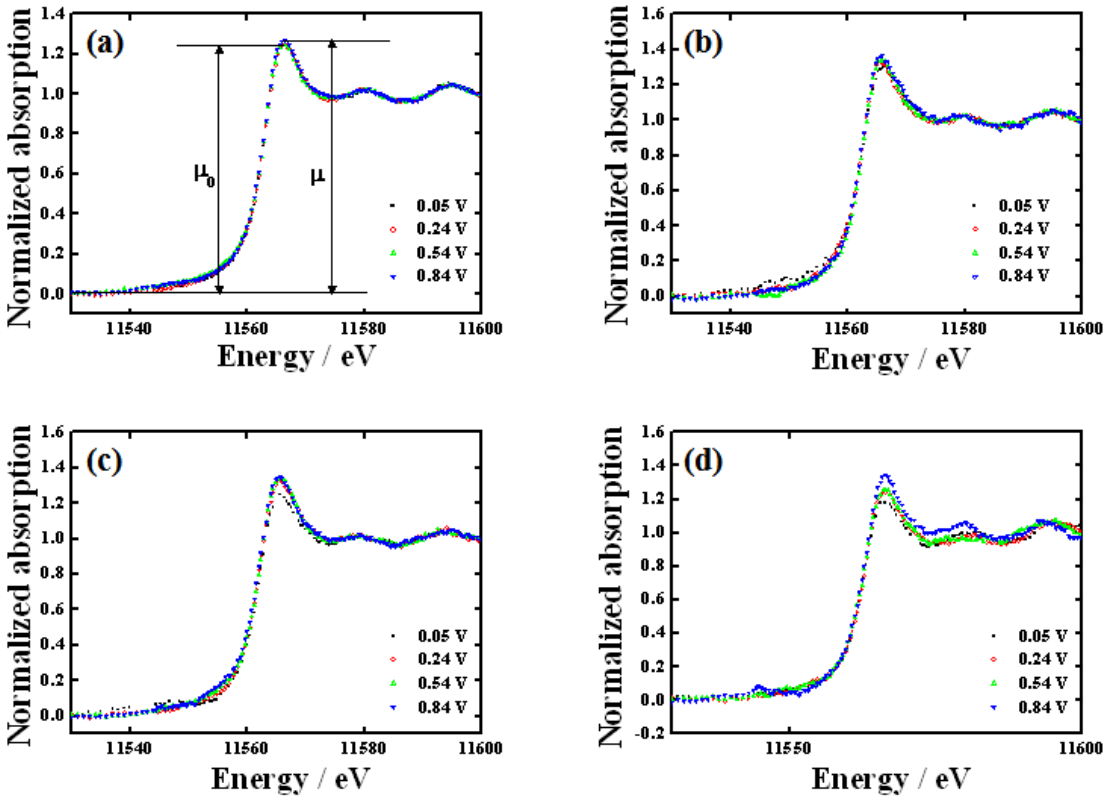

Figure S8. XANES at the Pt L_{III} edge for (a) 4 nm, (b) 3 nm, (c) 2 nm, and (d) 1.5 nm Pt/TiO_2 nanocatalysts in 0.1 M $HClO_4$ as a function of potential.

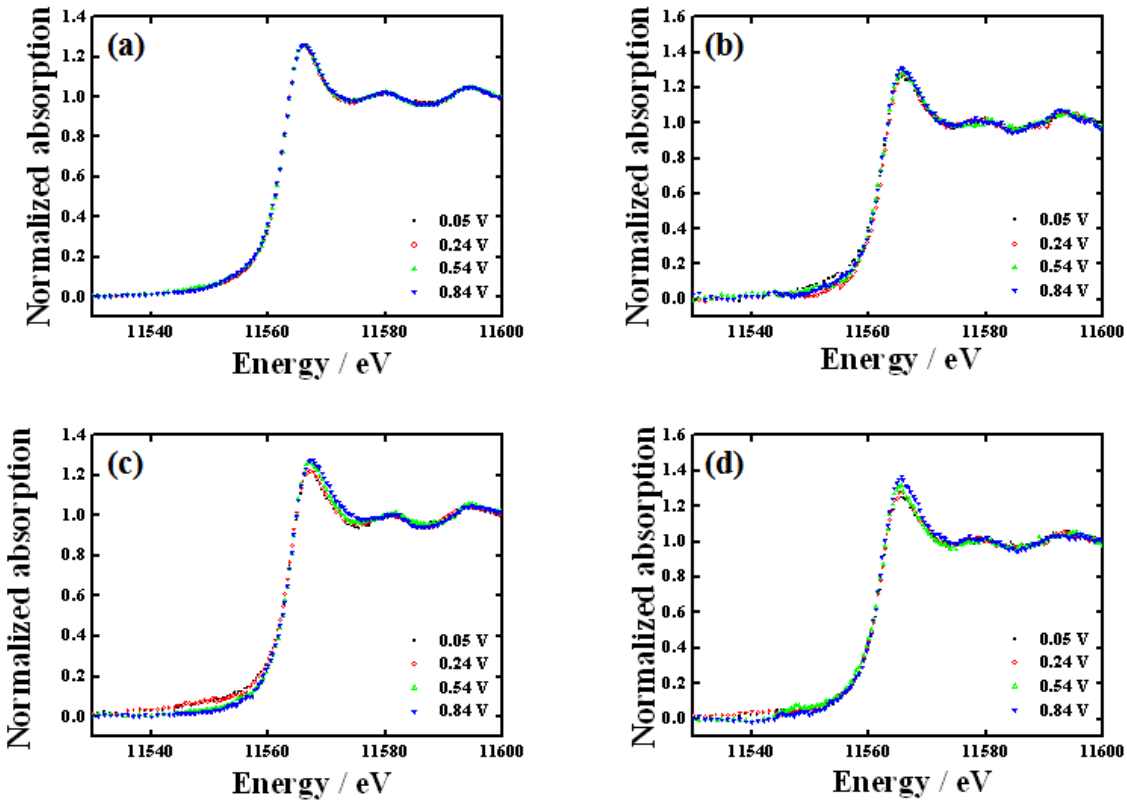

Figure S9. XANES at the Pt L_{III} edge for (a) 4 nm, (b) 3 nm, (c) 2 nm, and (d) 1.5 nm Pt/TiO_2 nanocatalysts in 0.1 M $HClO_4$ + 1 M CH_3OH as a function of potential.

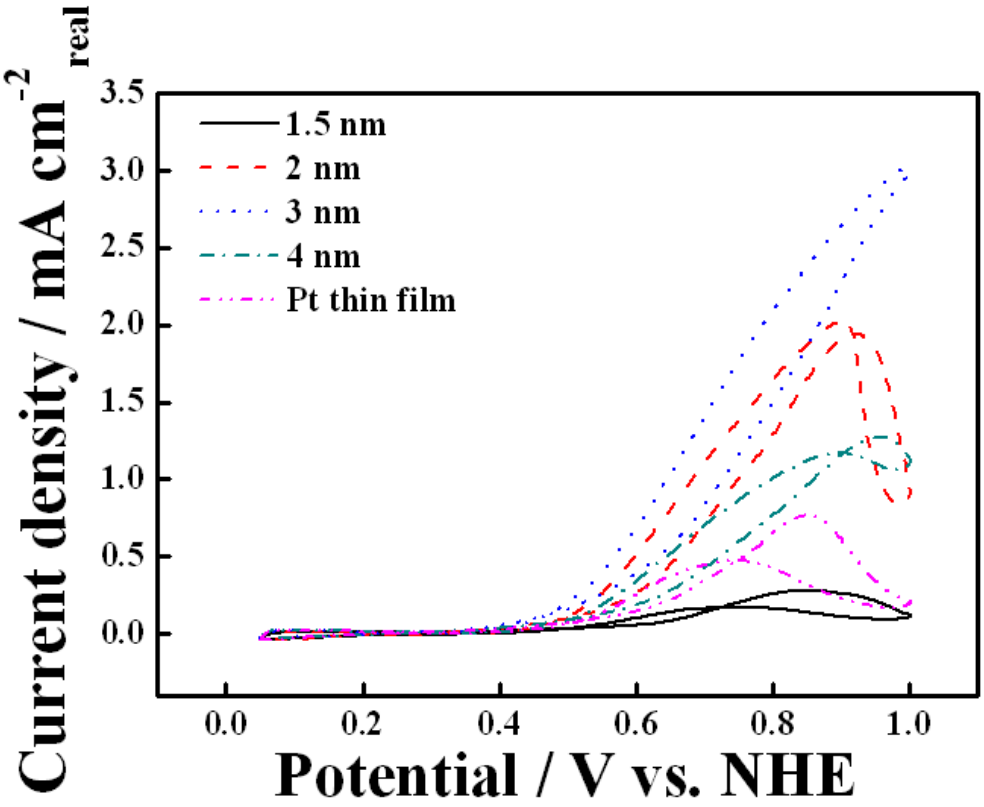

Figure S10. Polarization curves for the oxidation of methanol on 1.5 nm ~ 4 nm Pt/TiO_2 nanocatalysts deposited on the glass carbon electrodes in 0.1 M $HClO_4$ + 1 M CH_3OH at 298 K; sweep rate is 50 mV s^{-1}.

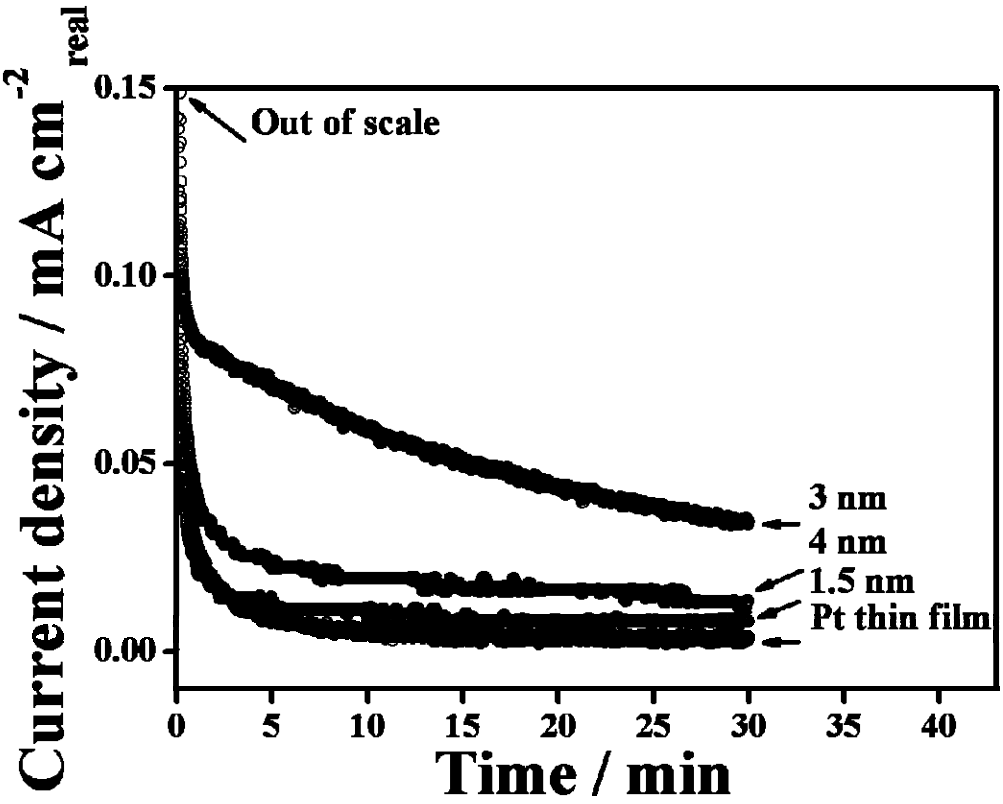

Figure S11. Chronoamperometry measurements of methanol oxidation at 0.5 V on 1.5 nm ~ 4 nm Pt/TiO_2 nanocatalysts deposited on the glass carbon electrodes in 0.1 M $HClO_4$ + 1 M CH_3OH at 298 K